Available online at www.sciencedirect.com

SCIENCE DIRECT®

ELSEVIER

Palaeogeography, Palaeoclimatology, Palaeoecology 230 (2006) 52–69

PALAEO

www.elsevier.com/locate/palaeo

Late Quaternary climate-induced lake level variations in Lake Petén Itzá, Guatemala, inferred from seismic stratigraphic analysis

F.S. Anselmetti [a,*], D. Ariztegui [b], D.A. Hodell [c], M.B. Hillesheim [c], M. Brenner [c], A. Gilli [a,c], J.A. McKenzie [a], A.D. Mueller [a]

[a] *Geological Institute, Swiss Federal Institute of Technology, ETH, Zurich, CH-8092 Zurich, Switzerland*
[b] *Institut Forel, Department of Geology and Paleontology, University of Geneva, Geneva, Switzerland*
[c] *Department of Geological Sciences, and Land Use and Environmental Change Institute (LUECI), University of Florida, Gainesville, 32611, USA*

Received 20 November 2004; received in revised form 14 June 2005; accepted 29 June 2005

Abstract

We used seismic images and sedimentary data from piston cores to conduct a sequence stratigraphic analysis of sediments in Lake Petén Itzá, northern Guatemala. Our results document lake level fluctuations in this lowland Neotropical region that were related to glacial-to-interglacial climate change during the Late Pleistocene. A bathymetric survey of Lake Petén Itzá (area = 100 km^2) revealed a maximum water depth of ~160 m and the existence of a deep cryptodepression that extends 50 m below modern sea level. The great depth suggests that the basin held water even during arid conditions associated with full glacial periods. Lake Petén Itzá may thus possess the only long continuous lacustrine sediment record of Late Pleistocene environmental and climate change in the lowland Neotropics. Two seismic reflection campaigns imaged the subsurface basin sediments that overlie basement. The sediment package was divided into four major seismic sequences (T, G, R, and B). Sequences are separated by unconformities that represent depositional cycles related to lake level fluctuations. Sediments of the uppermost sequence (T) were recovered and radiocarbon-dated in Kullenberg piston cores taken along a water depth transect. Seismic profiles reveal a basin-wide paleoshoreline just below sequence T at ~56 m below present lake level. This constructional feature formed during a lowstand of the last glacial period when the lake was reduced to only ~13% of its present volume. In cores taken landward of the paleoshoreline, Late Glacial-age deposits consist of paleosols, indicating subaerial exposure. Basinward of the shoreline, sediments are composed of dense gypsum sands and interbedded silty clays, reflecting authigenic gypsum formation under arid climate conditions. The top of the soil horizon and cessation of gypsum precipitation are represented by a strong seismic reflection (*t*). It marks the base of the uppermost seismic sequence T and is dated in several cores between ~11.1 and 10.2 cal kyr BP. Lake level rose quickly at this time in response to a shift from arid-to-humid climate conditions at the Late Glacial/Early Holocene transition. We infer a similar sediment response to climate variations in the older stratigraphic sequences (G, R, and B), related to earlier glacial-to-interglacial and stadial-to-interstadial cycles. Older sequences are also distinguished from one another by erosional unconformities that probably represent major lake level falls. Future recovery of the older stratigraphic

* Corresponding author. Tel.: +41 1 632 6569; fax: +41 1 632 1080.
E-mail address: flavio.anselmetti@erdw.ethz.ch (F.S. Anselmetti).

0031-0182/$ - see front matter
doi:10.1016/j.palaeo.2005.06.037

record by drilling in Lake Petén Itzá will provide ages for these older units and enable us to test the depositional model inferred from seismic stratigraphy.

Keywords: Paleoclimatology; Lake sediments; Seismic stratigraphy; Lake level changes; Guatemala

1. Introduction

Lake sediments are valuable archives of past environmental change on the continents. They can provide a continuous, sensitive record of changing conditions and processes that occur within the lake itself and in the surrounding catchment. Geophysical reflection seismic surveys provide quantitative data on sediment geometry, type, and stratigraphy, as well as depositional processes (Scholz, 2001, and references therein). In addition, seismic profiles are invaluable for choosing optimum locations for lake coring or drilling, especially in lakes with large lateral differences in sedimentation pattern. In closed basins that lack surface outflows, seismic stratigraphic analysis can be used to reconstruct past lake level fluctuations because such fluctuations control the lateral extent of seismic sequences, onlap relationships, and the occurrence of (subaerial) erosional surfaces and paleoshorelines (Scholz and Rosendahl, 1988; De Batist et al., 1996; Seltzer et al., 1998; Ariztegui et al., 2000; Gilli et al., 2001, 2005). Water level fluctuations in closed basins are mostly a function of the balance between precipitation and evaporation and thus leave a record of past climate changes. In addition to being regulated by the precipitation/evaporation ratio, water level fluctuations can be controlled by changes in subsurface inflows and outflows, particularly in karst areas. Wet/dry climatic alternations may also be recorded in the sediments of closed-basin lakes by varying amounts of evaporitic salts that are deposited as the lake volume expands and contracts (Piovano et al., 2002; Fedotov et al., 2004).

The objectives of seismic reflection studies dictate the choice of the seismic source to be used. High-frequency sources provide high-resolution data, but limit the depth of penetration. In contrast, lower-frequency sources penetrate to greater depth, but spatial resolution is compromised. Here we present results from a lacustrine seismic stratigraphic survey that used two seismic systems coupled with analyses of sedimentary piston cores that were collected along depth transects sited on seismic lines. The dual sources provided both high-resolution images of shallow subsurface deposits, and sufficient information on deep sediment layers, for sequence stratigraphic analysis. Integration of core analyses and seismic information permitted chronostratigraphic dating and correlation of lithologic changes with specific seismic reflections, and enabled us to develop a conceptual model for interpreting lacustrine depositional processes.

We applied a seismic stratigraphic approach to the sediments of Lake Petén Itzá, a large water body in the lowland Neotropics of northern Guatemala (Fig. 1), on the southernmost part of the Yucatan Peninsula. The lake has a surface area of 100 km^2 and lies at ~16°55′N, 89°50′W in the Department of Petén within the Petén Basin, an intra-cratonic basin located on the Maya block of the North American Plate (Fig. 2). The underlying stratigraphic section includes an up to 5-km thick sequence of Cretaceous to Tertiary deposits consisting of marine carbonates underlain by Jurassic continental sediments. A 1970 map of the geology of Guatemala [Mapa geológico de Guatemala, 1970, Instituto Geográfico Nacional (Guatemala)] indicates that Paleocene–Eocene marine carbonates are exposed at the surface surrounding the northern basin of Lake Petén Itzá, whereas Cretaceous carbonates characterize surface exposures to the south (Fig. 2). The lake basin occupies a large karst depression that follows a series of east–west aligned faults (Vinson, 1962). The northern shore of the lake is bounded by an inactive normal fault and marked by a steep karst ridge that follows the strike of the fault system, whereas the south shore is shelving, and in places rimmed by poorly drained seasonal swamps (*bajos*). Presently, Lake Petén Itzá's water is dilute (11.22 meq l^{-1}) and dominated by calcium and bicarbonate, with magnesium and sulfate following closely in concentration. Lake water pH is high (~8.0) and is saturated for calcium carbonate. There are abundant shells of

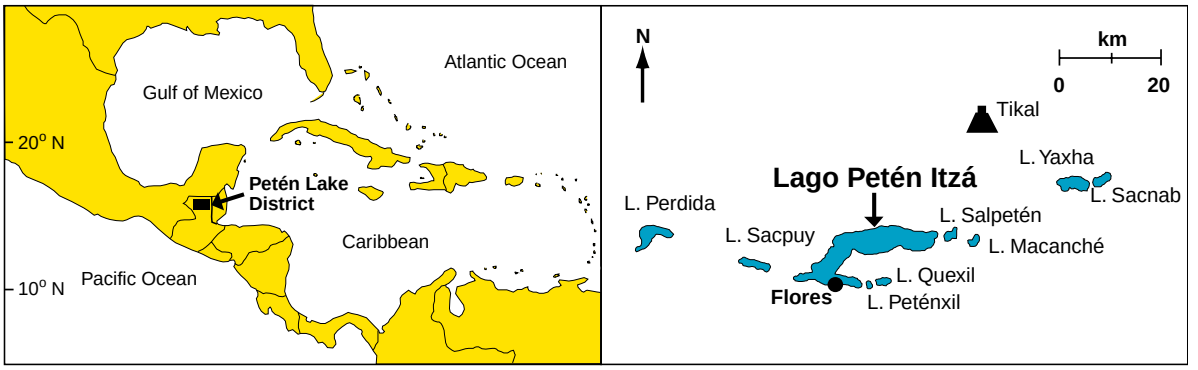

Fig. 1. Location of the Petén Lake District in northern Guatemala (left) and detailed map of the lakes and the location of the ancient Maya city of Tikal (right). Note the E–W alignment of the lakes.

carbonate microfossils (ostracods and gastropods) in the lake sediments (Covich, 1976; Curtis et al., 1998).

We produced the first bathymetric map for Lake Petén Itzá that shows a maximum water depth of ~160 m. The bathymetry is complex, reflecting the karst nature of the basement (Fig. 2). The modern lake surface is ~110 masl, which means the deepest part of the Petén Itzá basin is a cryptodepression that is ~50 m below present sea level. Today the lake is divided into a large main basin in the north (~30 km long and ~3–4 km wide) and a much smaller and shallower southern basin (14 km long and up to 1.5 km wide). A shallow sill connects the two. The north basin consists of several subbasins that may have been isolated during lowest lake level stands. Despite the lake's large size, water level has fluctuated appreciably (5–6 m) in the past few decades, flooding lakeside homes and businesses. Although Lake Petén Itzá is affected by subsurface leakage through the karstic bedrock, we believe that the climate-controlled precipitation/evaporation ratio has been more variable through time and thus exerts an important influence

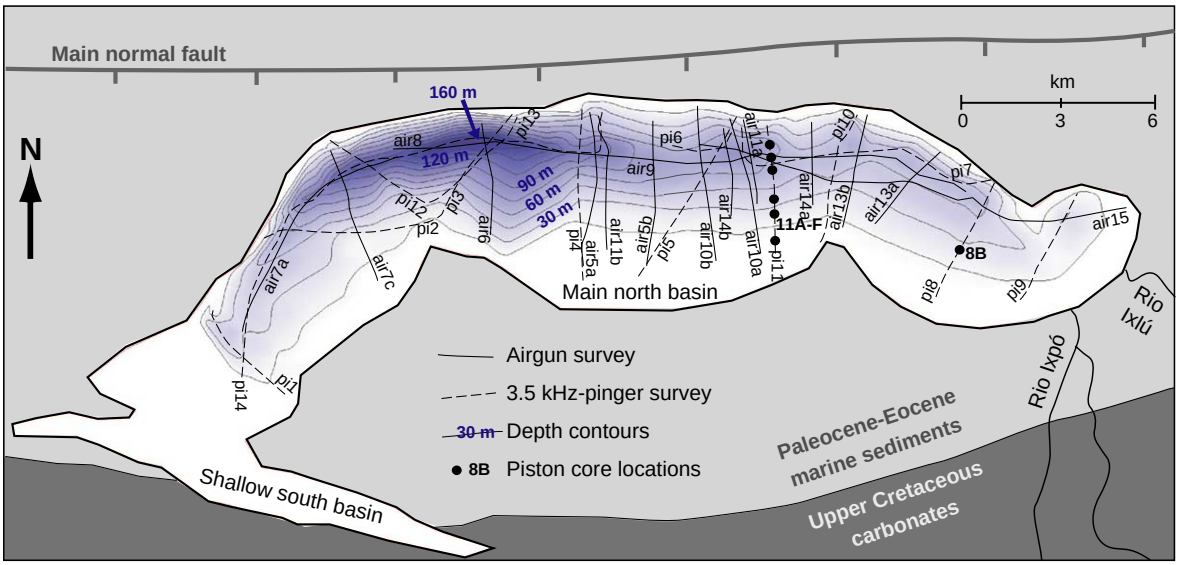

Fig. 2. Trackmap of all seismic lines in Lake Petén Itzá, superimposed on the interpolated bathymetric map (depth contours = 15 m). 3.5 kHz seismic survey (dashed lines) and airgun seismic survey (solid lines). Locations of Kullenberg piston cores taken along seismic lines pi11 and pi8 are indicated by dots. Geologic information (outcropping rock formations, track of the main normal fault) after Instituto Geográfico Nacional de Guatemala (1970). Two inflowing rivers are indicated at the eastern edge of the main basin.

on lake level changes. Most recent lake level fluctuations can be attributed to changes in the precipitation pattern of the 20th century (Deevey et al., 1980). Furthermore, variations in surface inflow as well as variations in subsurface in- and outflow are also strongly affected by climatically influenced surface water recharge. Consequently, climate acted as a major control on past lake level fluctuations.

Along with marine-based paleoclimate records from the Caribbean, terrestrial archives of past climate variations in Central America are of great interest for understanding the role of the tropics in the global climate system. Previous evidence from lake sediment records in the lowland Neotropics demonstrated that climate was drier during the last ice age than during the Holocene, and that most shallow lake basins in the region were dry in the Late Pleistocene (Deevey et al., 1980; Brenner et al., 2002). The termination of the Late Glacial and the transition into the Holocene has been studied in cores from Lake Miragoane, Haiti, and Lake Valencia, Venezuela, located on the northern and southern rim of the Caribbean, respectively. Both lakes were sufficiently deep to have held water and preserved sediment records during those time periods (Bradbury et al., 1981; Hodell et al., 1991; Curtis and Hodell, 1993; Brenner et al., 1994; Curtis et al., 1999). Older glacial-age lacustrine sediments from the region are rare and have been found in only a few deep basins in the Petén Lake District (e.g., Lake Quexil) of northern Guatemala (Deevey et al., 1983, Leyden et al., 1993, 1994). Lake Petén Itzá's great water depth made it resistant to desiccation. Thus, sediments in the deep north basin probably contain a long, continuous archive of latest Pleistocene paleoenvironmental change.

Based on seismic and core data, we present a conceptual model that relates changing sedimentation processes and sediment characteristics to presumed climate-induced lake level fluctuations in Lake Petén Itzá. The piston corer only retrieved the upper 6 m of Late Glacial and Holocene sediment, but the cores were sufficiently long to interpret the uppermost seismic sequence (Hillesheim et al., 2005). Drilling will be required to recover deeper, older deposits. Because of its great water depth (~160 m) and sediment thickness (>100 m), Lake Petén Itzá has been targeted for deep drilling by the International Continental Drilling Program (ICDP). Long cores from deep water will provide the stratigraphic sequences needed to recover the long paleoenvironmental archives that will be used to test the conceptual depositional model developed using cores and seismic stratigraphy.

2. Methods

Two seismic investigations of Lake Petén Itzá were undertaken in 1999 and 2002 including a shallow, high-resolution survey (3.5 kHz pinger) and a deeper, low-resolution survey (1 $in.^3$ airgun). The pinger survey provided seismic stratigraphic information for shallow subsurface sediments (<40 m), whereas the airgun survey provided images of deeper sediments and bedrock morphology for most of the lake basin. The acquisition parameters for both single-channel surveys are summarized in Table 1. Pinger data were processed by bandpass filtering (2–6 kHz) and gaining with a broad Automatic Gain Control (AGC; window length 100 ms). Airgun data were bandpass filtered (200–1000 Hz) and gained (AGC 200 ms). Next, a 1-3-1 trace mixing was applied to improve both lateral coherency of reflections and the signal-to-noise ratio. Positioning (GPS) accuracy of the airgun survey was on the order of ± 5 m, whereas accuracy of the earlier pinger survey in 1999 was lower, ± 50 m. Seismic data from both surveys were imported into interpretation software and a seismic stratigraphy was established. For calculation of the bathymetric map, an average water column velocity of 1500 m/s was assumed. The

Table 1
Parameters for the seismic surveys completed on Lake Petén Itzá in 1999 and 2002

Survey parameters	1999 campaign	2002 campaign
Source	Geoacoustic pinger	1 $in.^3$ Bolt airgun @ 70 MPa
Receiver	Geoacoustic pinger	20-element geopulse hydrophone
Frequency range (center frequency)	2–6 kHz (3.5 kHz)	200–1500 Hz (300 Hz)
Positioning (accuracy)	GPS (± 50 m)	GPS (± 5 m)
Boat speed	5 km/h	5 km/h
Recording format	SEG-Y	SEG-Y
Shooting interval	0.5 s	4 s
Maximum penetration	40 m	100 m
Vertical resolution	10 cm	1 m
Survey grid	80 km	90 km

maximum depth of the basin was confirmed during limnological sampling, when a water sampler was lowered to the bottom on a metered cable.

In June 2002, 13 piston cores were retrieved from 10 sites in Lake Petén Itzá's deep north basin. Piston cores were taken along selected seismic lines down to a water depth of 105 m. Retrieved sections included a transect of six cores on seismic line 11, ranging in water depth from 9.7 to 63.2 m. Cores were recovered using a Kullenberg-type piston corer triggered by a mud–water interface corer. In the laboratory, each core section was measured in its original polycarbonate liner for gamma ray attenuation (GRA) bulk density at 0.5-cm increments, using a GEOTEK Multi-Sensor Core Logger (MSCL). The instrument was calibrated at the start of each day using an aluminum and water stan-

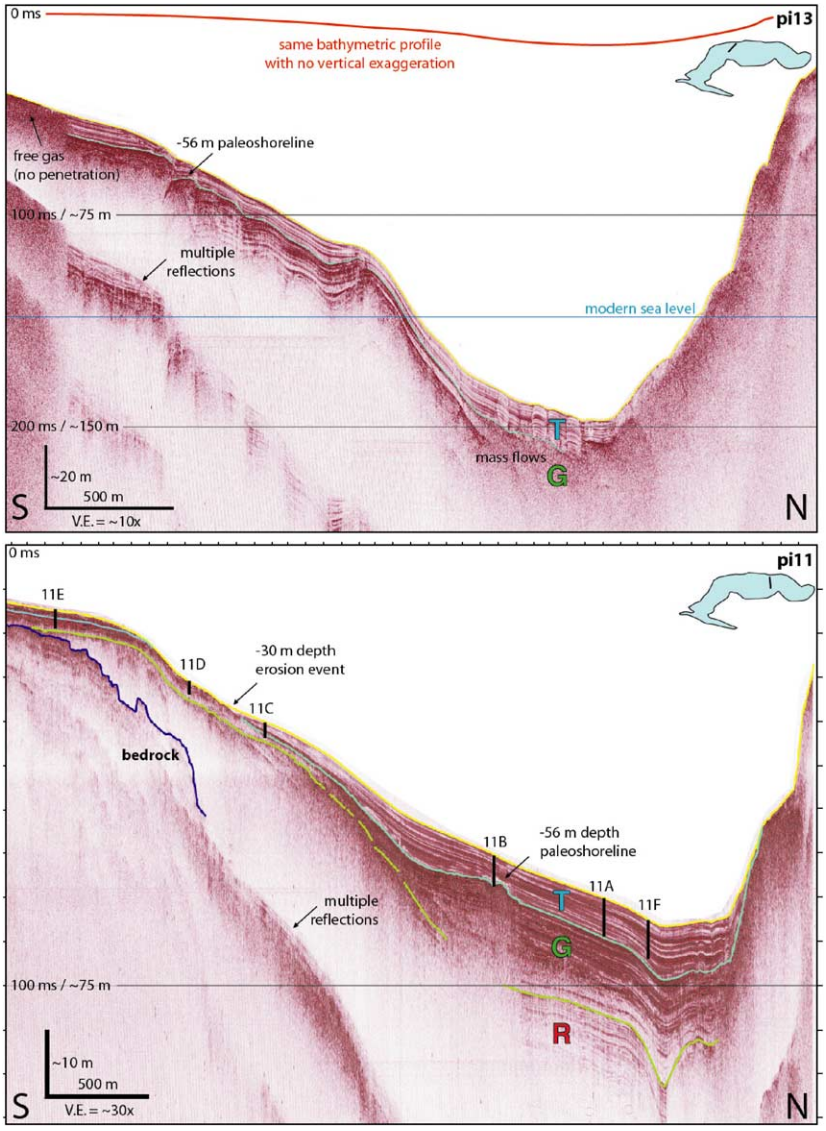

Fig. 3. 3.5 kHz seismic cross-sections pi13 (above) and pi11 (below). Line pi13 crosses the lake close to its deepest area. The red line at the top indicates the bathymetric profile of line pi13 with no vertical exaggeration. The locations of the Kullenberg core transect are indicated along line pi11. Small inset lake maps display locations of imaged seismic sections. The seismic sequences are labeled with capital letters.

dard. Split core sections were digitally imaged using a GEOSCAN III linescan camera linked to the MSCL. The cores were tied to the seismic data with a depth–time conversion assuming an acoustic velocity of 1500 m/s (measured as average MSCL-velocity). Subsequently, the cores were split, described and sampled for radiocarbon dating (Hillesheim et al., 2005). All radiocarbon ages, given in calendar years before 1950 (cal kyr BP), were measured on terrestrial organic material and calibrated with INTCAL98 (Stuiver and Reimer, 1993; Stuiver et al., 1998) unless explicitly stated otherwise.

On August 13 2002, we measured temperature in the water column using a Sea-Bird SBE 19 SEACAT CTD-sonde (Conductivity, Temperature, Depth) that was lowered to the lake floor at the deepest point (~160 m) of Lake Petén Itzá (position: 17°0.416′N, 89°50.791′W).

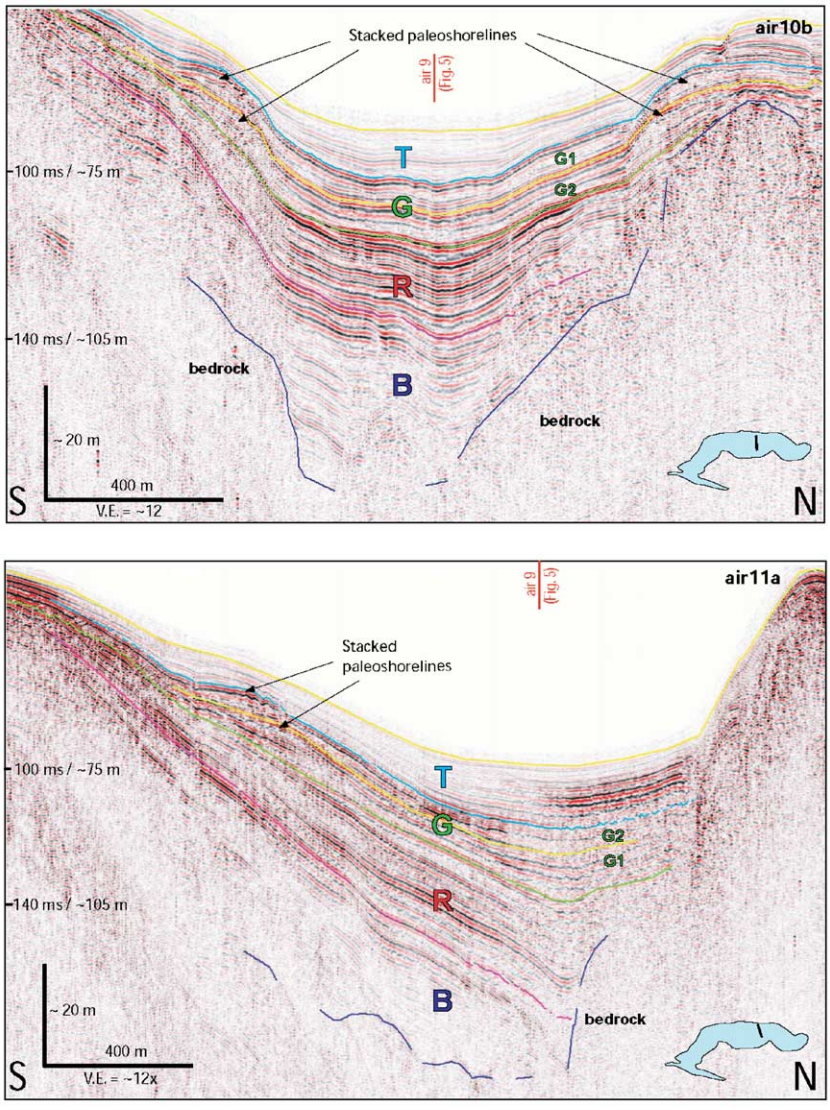

Fig. 4. Airgun seismic cross-sections air10b (above) and air11a (below). Small inset lake maps display locations of imaged seismic section. The seismic sequences are labeled with capital letters. The intersection with E–W line air9 (Fig. 5) is marked on the top of each plot.

3. Results

3.1. Seismic stratigraphy

We analyzed both the 3.5 kHz and airgun seismic dataset using standard seismic sequence stratigraphic concepts (Vail et al., 1977) and identified four major seismic sequences overlying acoustic basement. Each sequence is bounded by an unconformity or its correlative conformity. Seismic stratigraphic analysis of the entire sediment package was done only for the central and eastern areas of the lake, because high concentrations of gas in sediments at the western end of the basin prevented acoustic penetration to bedrock. Because of its shallow-water depth, the southern basin was not surveyed with the airgun source. Figs. 3 and 4 display N–S seismic cross-sections of the lakebed acquired with the 3.5 kHz and airgun sources, respectively. Fig. 5 shows an airgun seismic section running parallel to the long axis of the basin, in an E–W direction. The four depositional sequences of the section are labeled from top to bottom (Fig. 4). Capital letters indicate the color used to illustrate the seismic reflection that marks the underlying sequence boundary, i.e., T(urquoise), G(reen), R(ed) and B(lue). The following describes the seismic geometries and seismic facies of each sequence:

3.1.1. Sequence T

Sequence T is the youngest sequence, and is characterized by highly continuous, low-amplitude reflections with a few internal reflections displaying higher amplitudes locally (Fig. 3). Within the sequence, however, no major horizons stand out prominently, nor are there any consistent unconformities. The base of Sequence T is defined by a high-amplitude reflection that is onlapped by younger strata that comprise the low-amplitude seismic facies of Sequence T. Sequence T is thickest in the deeper parts of the basin, reaching a maximum thickness of about 10–15 m (Figs. 3 and 4). In a few areas, local mass movements that mobilized Sequence T sediments are recognized by erosive scar surfaces and associated seismically chaotic-to-transparent flow deposits (Fig. 6). Along the gently-dipping southern shore, Sequence T consistently wedges out on the modern lake floor at a water depth of ~30 m, where it displays upslope thinning and gradual condensation of reflections (Fig. 7A). In one case, the disappearance of Sequence T in this depth range is clearly associated with erosional processes as even the top of the underlying Sequence G is slightly eroded (line pi8; Fig. 7A). This disappearance of Sequence T at −30 m can be mapped all along the southern shore of Lake Petén Itzá (Fig. 8). Further upslope, in water depths <15 m, where slope angle decreases, Sequence T sediments

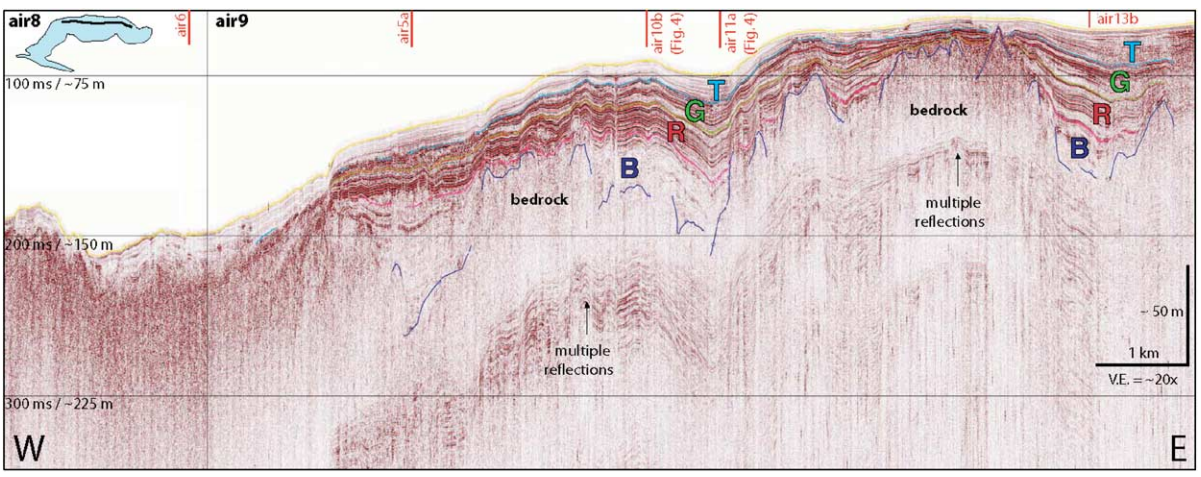

Fig. 5. Basin-parallel airgun cross-sections composed of two seismic lines, air8 and air9. Small inset lake map displays location of imaged seismic track. The seismic sequences are labeled with capital letters. The intersections with other airgun seismic lines are marked at the top of the plot.

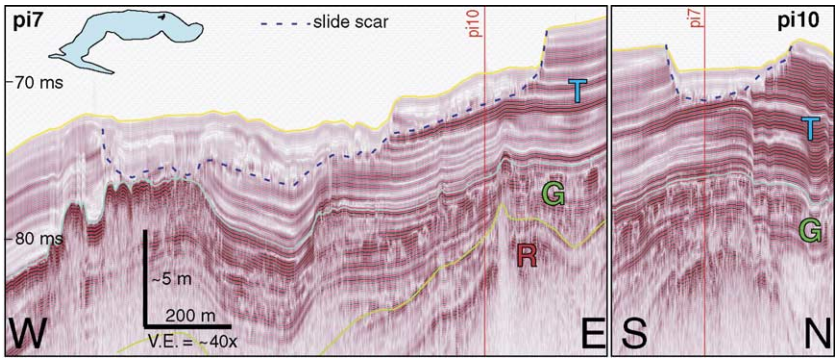

Fig. 6. Example of a massflow within Holocene sequence T. Two perpendicular seismic lines (pi7 and pi10) cut a headwall scar surface (marked as dashed line). The scar surface is partly infilled by chaotic and deformed sediments that slid away. Small inset lake map displays location of imaged seismic lines. The seismic sequences are labeled with capital letters.

reappear. It is impossible, however, to trace reflections from shallow to deep water across the erosional zone. Identification of the correlative boundary at the base of Sequence T in shallow-water is based mainly on correlation among cores taken along seismic line pi11 (Fig. 3, see also Fig. 10).

3.1.2. Sequence G

The underlying Sequence G also displays continuous reflections but with higher amplitudes than in Sequence T (Figs. 3 and 4). Some areas show transparent-to-chaotic seismic facies, indicating local mass movements. Along the gently-dipping southern edge of the basin, the top of Sequence G is characterized by a rugged morphology and/or erosion feature that occurs consistently at a depth of ~56 m below lake surface (Fig. 7B). This feature can be traced around most of the Petén Itzá basin (Fig. 8). In most cases, this feature is characterized by an accumulation of sediment that is up to 3 m thick and ~100 m wide, which formed atop a substrate of constantly-dipping slope sediments. It usually displays steep basinward sides and more gently sloping landward flanks (Fig. 7B). On the airgun seismic lines, the constructive feature peaking at ~−56 m is imaged as a stacked succession of two sediment build-ups that divide Sequence G into two subsequences, G1 and G2 (marked on Fig. 4).

Sequence G becomes thicker in the deeper parts of the basin, attaining a maximum thickness of ~20 m. Increased thickness is attributed, in part, to sediment that accumulated as a consequence of mass movements in the profundal zone of the basin. Similar to Sequence T, slide scars associated with these mass movements can be mapped on the steeper parts of slopes.

3.1.3. Sequence R

The overall seismic character (facies and geometries) of Sequence R is very similar to Sequence G. The R/G sequence boundary is defined by an erosional unconformity in water depths between ~30 and 40 m, and is best illustrated on seismic lines pi11 (Figs. 3 and 7A) and pi8 (Fig. 7A). The basinal part of Sequence R consists of a highly continuous seismic facies, whereas the upslope part lacks lateral coherency of reflections. Sequence R is slightly thicker than G in places, reaching a maximum thickness of about 30 m.

3.1.4. Sequence B

Sequence B is the oldest sedimentary sequence and displays the most complex seismic facies architecture. In particular, the longitudinal airgun seismic section (Fig. 5) illustrates how the geometry of B differs from the overlying sequences. In some areas, it attains a thickness of 50–60 m, especially where it infills and onlaps topographic lows of the underlying basement. Its seismic facies is more chaotic, with occasional high-amplitude reflections, but it also shows areas that are seismically stratified. Sediments of Sequence B are mostly restricted to the deepest bedrock depressions, while equivalent sediment on basement highs is either condensed or absent.

3.1.5. Acoustic basement

Acoustic basement is recognized in most shallow areas and in the eastern-to-central areas of the deep

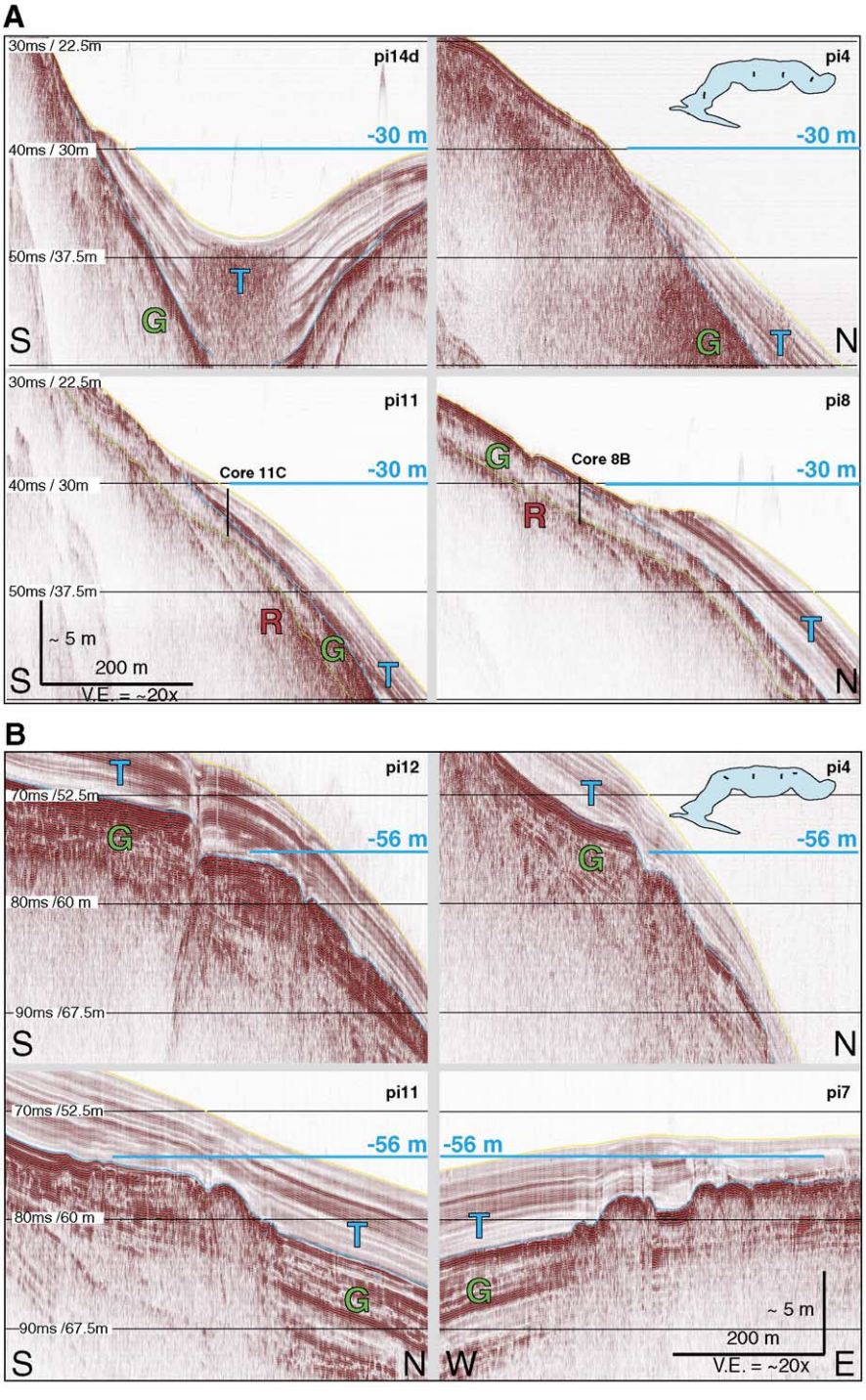
A
30ms / 22.5m
pi14d
-30 m
40ms / 30m
50ms /37.5m
T
G
S
pi4
-30 m
G
T
N
30ms / 22.5m
pi11
Core 11C
-30 m
40ms / 30m
50ms /37.5m
R
G
T
~ 5 m
200 m
V.E. = ~20x
S
pi8
G
Core 8B
-30 m
R
T
N
B
T
pi12
70ms /52.5m
G
-56 m
80ms /60 m
90ms /67.5m
S
pi4
T
G
-56 m
N
pi11
70ms /52.5m
-56 m
80ms /60 m
T
G
90ms /67.5m
S
N
pi7
-56 m
T
G
~ 5 m
200 m
V.E. = ~20x
W
E

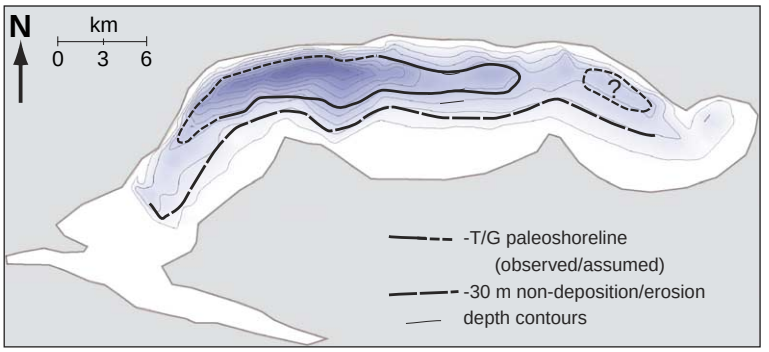

Fig. 8. Map of paleoshoreline and erosion/non-deposition features superimposed on modern bathymetry. The shoreline features at ~−56 m water depth associated with the G/T sequence boundary (observed: solid line; assumed: dashed line) shows the size of a paleolake with reduced volume. A second, separate lake may have existed in the eastern part of the basin. The ~−30 m erosion/non-deposition event can be mapped along the south shore of the lake (long-dashed line) and may be a consequence of water column circulation down to the metalimnion.

basin. Basement was not imaged in the central-to-western parts of the deep basin because gas limited penetration of the seismic signal (Fig. 5). In general, the basement surface is highly irregular, showing numerous basins and elevated areas (Fig. 5). Along the southern shore, a series of apparently basin-parallel faults are recognized on the airgun lines (Fig. 9). These faults are expressed as a series of basement blocks that show a stepwise decline in elevation toward the north. The irregular basement morphology is not expressed by the modern lake floor topography because sediments, particularly of sequence B, have smoothed out many of the basement irregularities.

3.2. Core-to-seismic correlation

The seismic stratigraphic architecture of uppermost sequence T was linked to dated sediment lithologic changes using piston cores that were taken at selected locations on 3.5 kHz seismic lines. Six Kullenberg piston cores, ranging in water depth from 9.7 to 63.2 m, were recovered along a N–S transect on seismic line pi11 (Figs. 3 and 10). The longest core recovered was 6.0 m and all cores, except 11F, penetrated the base of seismic Sequence T. Core-to-seismic correlation was accomplished by comparing seismic reflection profiles to gamma ray attenuation (GRA) bulk density of the piston cores, assuming a constant sediment velocity of 1500 m/s (Figs. 10, 11).

In shallow-water cores 11C-E (<30 m water depth), the G/T boundary is marked by an upcore decrease in density, from ~1.9 to ~1.3 g cm^{-3} (Fig. 10). This boundary represents a lithologic transition from a dark-colored, organic-rich paleosol to partially-laminated lacustrine sediments composed predominantly of biogenic carbonate with varying amounts of organic matter and clay (Hillesheim et al., 2005). The top of the soil horizon is dated at 11.1, 10.7 and 10.2 cal kyr BP in cores 11C (30 m water depth (wd)), 11D (20.9 wd), and 11E (9.7 m wd), respectively. In deep water cores 11A and 11B (>51.6 m wd), the lithologic change associated with this sequence boundary occurs at 5.1 and 5.3 m, respectively. At these levels, density decreases upcore from ~1.7 to ~1.4 g cm^{-3}, marking a lithologic change from dense gypsum sands and interbedded silty clays, to sediment dominated by calcium carbonate and organic matter with varying amounts of

Fig. 7. A: The erosional/non-depositional event at ~−30 m depth is seen on the 3.5 kHz data along the entire south shore of the lake. Lines pi14d, pi4, and pi11 display rather condensed sedimentation above that depth, whereas line pi8 shows signs of erosion. Fig. 8 shows track of this feature in map view. Small inset lake map displays locations of the four imaged seismic tracks. The seismic sequences are labeled with capital letters. B: The ~−56-m depth paleoshoreline is seen on the 3.5 kHz data along the entire lake. This turquoise unconformity (base of Sequence T) indicates a lake level lowstand that created either erosional coastal notches (two upper examples) or accumulations of (evaporitic?) shore mounds (two lower examples). Fig. 8 shows track of this feature in map view. Small inset lake map displays the location of the four imaged seismic tracks. The seismic sequences are labeled with capital letters.

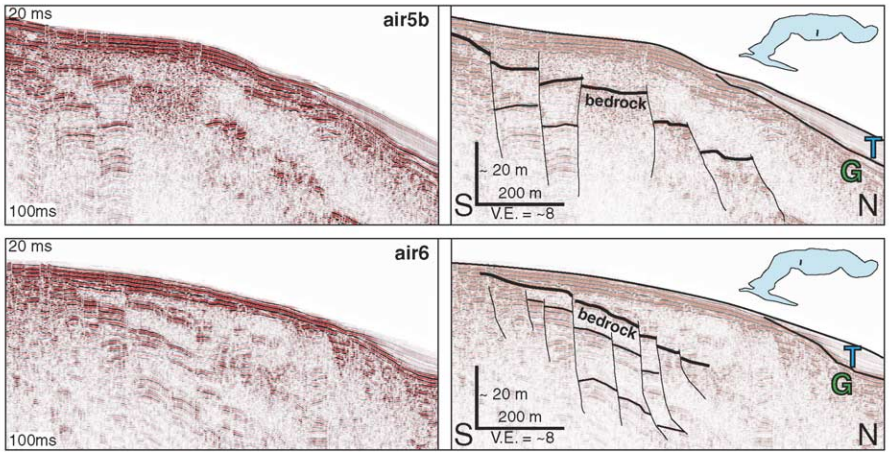

Fig. 9. Uninterpreted (left) and interpreted (right) versions of airgun seismic lines air5b and air6, imaging the southern area of the main basin (small lake map insets display location of seismic tracks). The two seismic lines document the bedrock structures along the gently-dipping, shallow south lake shore. Bedrock, outcropping onshore to the south, steps down northward in a series of basin-parallel normal faults. Together with the very steep north shore (half-graben geometry), these observed structures support the argument for a tectono-karstic origin of the lake.

detrital clay. The age of this transition is ~10.7 cal kyr BP, marking the boundary between the Late Glacial and Holocene Periods (Hillesheim et al., 2005). In all cases, the prominent upcore decrease in bulk density yields a strong, high-amplitude reflection marking the G/T sequence boundary (Fig. 11).

Core 11A (58.2 m wd) penetrated the base of sequence T basinward of the previously described sediment mound, whereas the base of Core 11B (51.6 m wd) sampled this horizon at the top of this constructional sediment feature (Fig. 11, line pi11). Despite the different coring locations and sediment geometries, the bases of both cores terminated in the top of underlying Sequence G in gypsum-rich sediments. In shallow-water cores 11C, 11D, and 11E, 1–1.5 m of Sequence G sediments were recovered. They consist of mottled to partially-banded, clay- and carbonate-rich lacustrine sediment. Basal ages of cores 11C, 11D, and 11E are 31.0, 20.7, and 15.9 ^{14}C kyr BP, respectively (Fig. 10; uncalibrated AMS ages; Hillesheim et al., 2005). Core 11C contains the most condensed section of Sequence G, as it possesses the oldest basal age (Fig. 10).

In addition to the cores along seismic line pi11, core 8B was taken in 27.3 m of water on seismic line pi8, in an area where most of Sequence T is missing due to removal by downslope mass movement (Fig. 7A). This core evidently penetrated both the G/T and the R/G sequence boundaries and recovered what may be the oldest sediment sampled by the Kullenberg corer. The base of Sequence G in core 8B corresponds to an upcore decrease in density from ~2.3 to ~1.8 g cm^{-3} near the base of the core (~254 cm). The lowermost 6 cm of core 8B consist of large, dense gypsum nodules that are overlain sharply by a shell hash layer composed of large gastropods. The shell layer grades into a silty lacustrine clay with varying degrees of laminations. At 90 cm in core 8B, this lacustrine sequence is capped by a paleosol, which coincides with the top of Sequence G (Fig. 7A). Bulk density decreases upcore across the paleosol, from ~1.8 to ~1.5 g cm^{-3}, similar to the pattern seen in shallow-water cores on seismic line 11A. This transition marks the onset of lacustrine carbonate sedimentation following subaerial exposure.

4. Discussion

The sequence stratigraphic architecture in Lake Petén Itzá indicates that this lacustrine system was strongly influenced by a fluctuating lake level that was, in turn, predominantly controlled by climate fluctuations. By integrating seismic and core results in the upper seismic sequence T, we developed a conceptual model for how sediment lithologies and

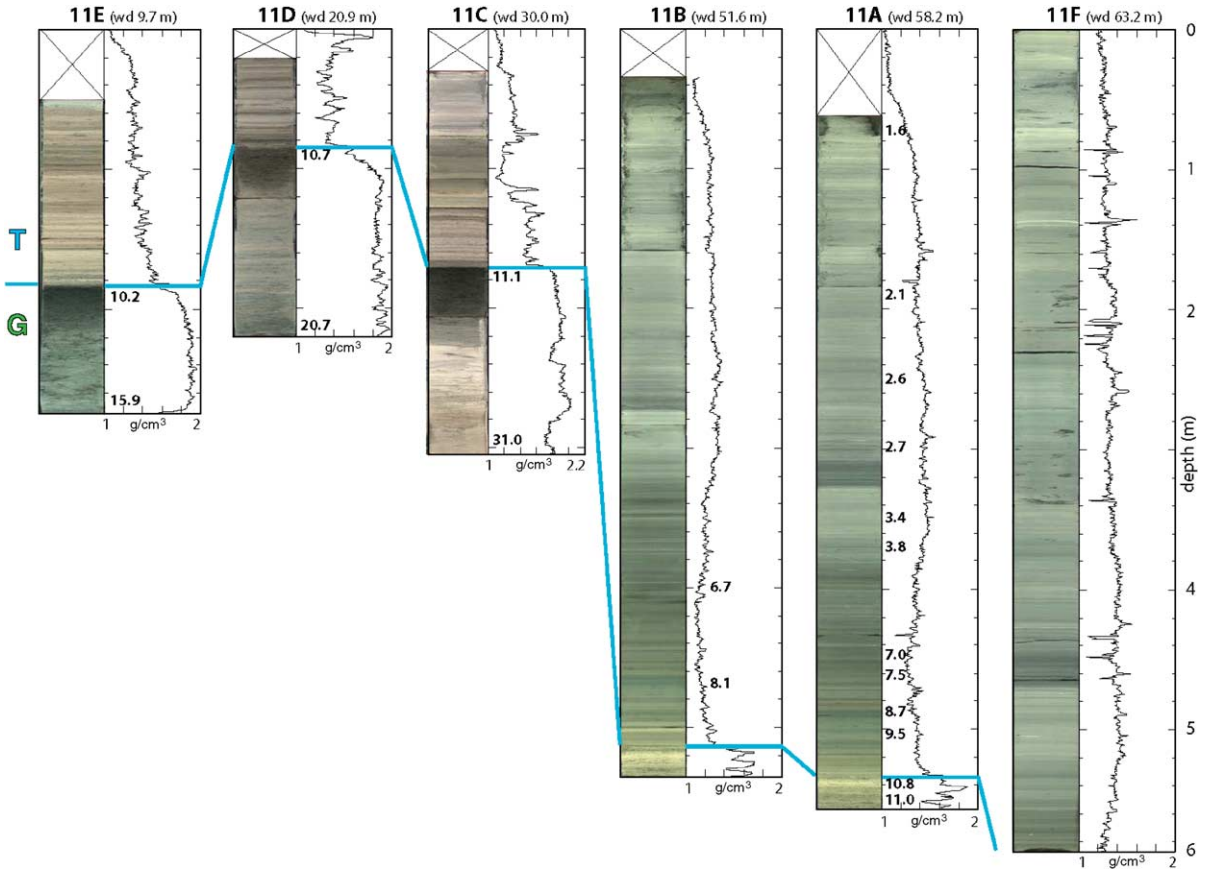

Fig. 10. Photographic images and bulk density of Kullenberg cores taken along a water depth transect on seismic line pi11 (Fig. 3). Photographs were stretched horizontally to better illustrate the stratigraphy (all cores are 6 cm wide). Missing uppermost sections of the long cores are indicated by crosses at the top of the columns, but were recovered with a mud–water interface corer). Note the consistent density increase moving downward across the turquoise T/G sequence boundary (Holocene/Late Glacial transition), reflecting the dark-colored soil horizon in cores 11E, D, and C and the light-colored gypsum deposits in cores 11B and A, both overlain by Early Holocene lacustrine sediments. Radiocarbon ages in cal kyr BP are marked at sample locations and are all calibrated except for basal dates in cores 11C, 11D, and 11E that are uncalibrated ^{14}C dates on shell material (Hillesheim et al., 2005).

geometries responded to climate-induced variations in lake level during the Late Glacial and Holocene. These concepts were then extrapolated to the deeper seismic sequences to interpret the older paleoenvironmental history of the basin.

Sequence T thins or wedges out consistently in water depths of 30 m throughout the basin, indicating modern erosion or non-deposition occurring around that water depth (Fig. 7A). There is, however, no historical evidence for a −30 m lake level lowstand that would be required to explain this feature if it were formed by subaerial erosion. In addition, Sequence T reappears in water depths shallower than 15 m and an almost continuous Holocene section was recovered in a water depth of 7.6 m (Curtis et al., 1998). If not eroded or reduced by subaerial exposure, this feature must be related to physical limnetic processes. The 30 m isobath corresponds to the base of the thermocline in Lake Petén Itzá (Fig. 12), and erosion/non-deposition may be related to internal progressive waves at the metalimnetic interface, as described in other large lakes (Lemmin, 1998). Although only one CTD measurement was obtained from Lake Petén Itzá in August 2002, it is probably representative of limnetic thermal structure throughout most of the year because seasonal temperature changes are small.

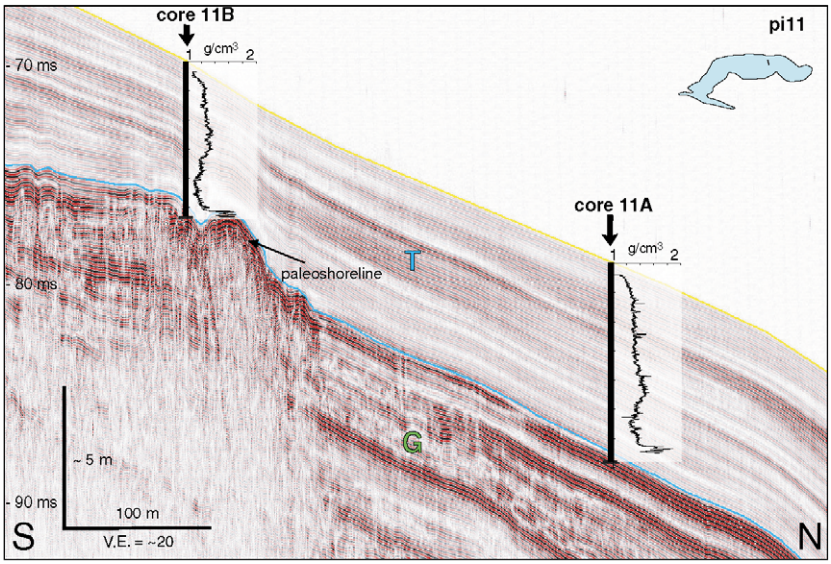

Fig. 11. Superposition of Kullenberg cores 11A and 11B along seismic line pi11 (assuming an acoustic velocity of 1500 m/s). The density contrast at the Late Glacial–Holocene transition results in a high-amplitude reflection (G/T sequence boundary = turquoise line). Small lake inset maps display locations of imaged seismic tracks. The seismic sequences are labeled with capital letters.

No prominent unconformities occur within Sequence T, indicating that environmental changes were small during the Holocene, at least relative to the large fluctuations associated with the Late Glacial lowstand. Much of Sequence T consists of a thick detrital clay unit ("Maya clay") that has been identified in many Petén lakes, and attributed to accelerated soil erosion resulting from ancient Maya land clearance (Deevey et al., 1979; Binford et al., 1987; Brenner, 1994; Rosenmeier et al., 2002).

The morphologic feature found throughout the basin at ~−56 m water depth is interpreted to be a paleoshoreline that formed during the end of the last glaciation. This lake level lowstand represents an ~87% (4.8 km^3) reduction in water volume relative to today (Hillesheim et al., 2005; Fig. 8). This interpretation is supported by both the feature's constant depth of occurrence and its morphology, which is similar to that of lacustrine shorelines in other closed lake basins (Thompson, 1992; Adams and Wesnousky, 1998; Ibbeken and Warnke, 2000; Komatsu et al., 2001; Sack, 2001; Gilli et al., 2005). The top of the paleoshoreline coincides with the G/T sequence boundary mapped on the seismic sections. Piston core 11B sampled the top 20 cm of the paleoshoreline and

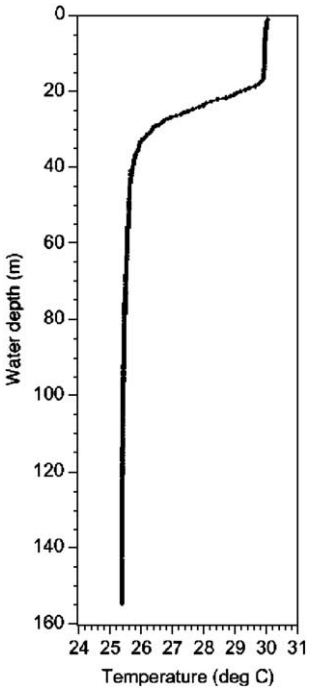

Fig. 12. CTD profile of temperature taken on 13 August 2002 at the deepest point of Lake Petén Itzá. Note the thermocline between ~20 and 35 m water depth.

recovered dense gypsum sands interbedded with silty clays. Rather than classic beach gravels found along other lake shores, which form at or just above lake level, the paleoshorelines of Lake Petén Itzá may represent subaquatic littoral depocenters of evaporites. Usually, such subaquatic shoreline formation is attributed to sediment redeposition through strong winds, currents, and waves (Wattrus and Rausch, 2001). In this case, precipitation of gypsum may have occurred in the shallow littoral areas where water temperatures were high and evaporation intense. In fact, calculations based on water chemistry indicate that Lake Petén Itzá would be saturated for $CaSO_4$ if lake volume were reduced by 87%. The observed drowned paleoshoreline structures would develop following a subsequent lake level rise.

Landward of the paleoshoreline in cores 11C–E, the sequence boundary coincides with a subaerial exposure surface (i.e., paleosol), whereas basinward, gypsum–clay lithologies persist to the water depth of Core 11A, i.e. 58.2 m. The G/T transition has yet to be recovered in cores from the deeper basin. The sequence boundary was consistently dated to between 10.2 and 11.1 kyr in all five cores retrieved along seismic line 11 (Fig. 10).

The Late Glacial lowstand of Lake Petén Itzá is consistent with inferences based on cores retrieved from nearby Lakes Quexil and Salpetén that also indicated lake level lowering of 30–40 m during the last glacial period (Deevey et al., 1983). Given their modern maximum water depths of just over 30 m, those lakes were probably ephemeral during the Late Glacial. Similar to deep water cores taken in Lake Petén Itzá, glacial-age sediment in Lakes Quexil and Salpetén was also dominated by gypsum and clay, indicating more saline conditions than today. Glacial-age vegetation consisted of sparse temperate thorn scrub and taxa such as *Juniperus*, reflecting an arid climate with estimated temperatures of ~6.5 to 8 °C lower than present (Leyden et al., 1993, 1994).

Landward of the paleoshoreline, the G/T sequence boundary represents a transgressive surface, in which paleosols are overlain by lacustrine deposits. At ~10.3 cal kyr BP, near the Pleistocene/Holocene boundary, climate became more mesic and Lake Petén Itzá filled rapidly. Shortly after 10.2 cal kyr BP, the lake had risen to within 8–10 m below the modern level as documented by the resumption of lacustrine deposition in core 11E (9.7 m water depth) and core 6-VII-93 taken in Petén Itzá's southern basin (8 m wd) (Curtis et al., 1998).

The integration of sediment core and seismic data provides a conceptual model that can be used to explain how lake level and related sedimentation processes in Lake Petén Itzá responded to climate change. Glacial-to-interglacial variations in lake level controlled the pattern and lithologies of sediments deposited in the basin. Full glacial periods were marked by low lake level that caused subaerial erosion and development of paleoshoreline features. The related unconformity defines a sequence boundary that can be traced on seismic profiles from shallow to deep water where it ultimately becomes conformable. Landward of the glacial paleoshoreline, soils developed, whereas gypsum was precipitated basinward of the paleoshoreline, a sedimentologic response seen in other closed-basin lakes (Piovano et al., 2002; Fedotov et al., 2004). Full or intermediate interglacial conditions were characterized by higher lake level, giving rise to lacustrine sediments with draping geometries, which overlie the sequence boundary with transgressive basal sediments. These highstand sediments consist of varying proportions of biogenic carbonate, organic matter, and detrital material. A typical seismic sequence is confined by two unconformities and consists of sediment deposited during both a lowstand and highstand of a lake level cycle, likely produced by orbital-scale climate fluctuations (e.g., marine isotope stages). Higher-frequency lake level fluctuations are superimposed upon these long-term cycles, but cannot be resolved on seismic sections. These shorter duration events are expressed by small-scale lithologic changes (Hillesheim et al., 2005) that may produce high-amplitude reflections such as those seen within Sequences G and R (Figs. 4 and 5).

We applied this depositional model to seismic stratigraphic units G, R, and B to interpret the older sediment record. The R/G sequence boundary is characterized by a prominent erosional unconformity that generally occurs in 30–40 m water depth, representing a previous low lake stage (Figs. 3 and 7A). Although the R/G unconformity has not been dated directly, it must be older than the basal date of core 11C (31 ^{14}C kyr BP; measured on carbonate material) that failed to penetrate the R/G sequence boundary. We speculate that the R/G sequence boundary represents an erosional phase associated with a low lake stage, and

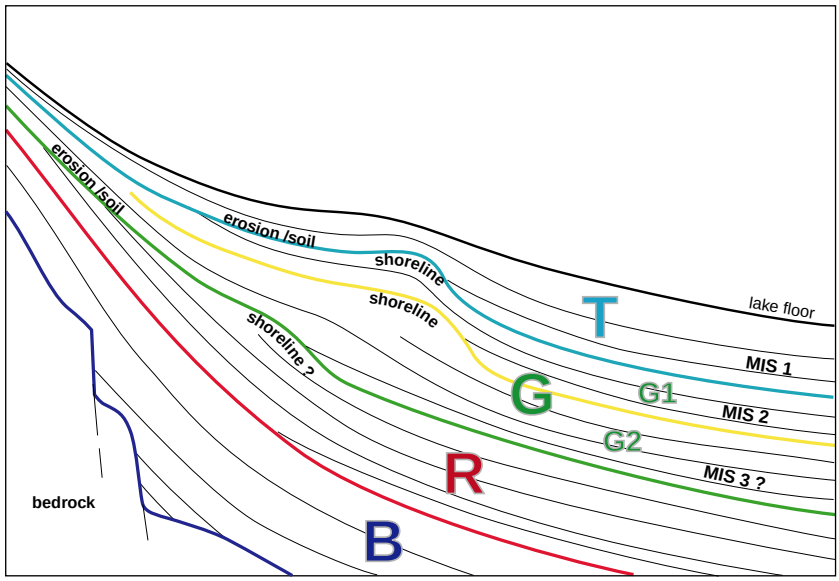

Fig. 13. Schematic summary of the sequence stratigraphic architecture of Lake Petén Itzá sediments that is related to past lake level fluctuations. Also indicated are confirmed and postulated (?) correlations with ages of marine oxygen isotope stages (MIS).

could be as old as the MIS4/3 boundary (Fig. 13). Under this assumption, Sequence G was deposited during MIS 2 and 3, whereas Sequence R could represent MIS 4 and older deposits. The occurrence of the two stacked paleoshoreline succession G1 and G2, which are not separated by a significant high-stand tract, could represent two rapid successive events of low lake level. Because it is assumed that the basin was not affected significantly by neotectonism, the accommodation space for the younger of the stacked shorelines must have been created by a rising lake level. This, however, could not have been a gradual transition (i.e. a continuously rising lake level), because the two paleoshorelines are clearly separated in the seismic data by a high-amplitude reflection (Fig. 4). Together with other high-amplitude reflections within Sequence G, they may reflect greater frequency of lithologic changes corresponding to the rapid stadial–interstadial oscillations of MIS 3 (i.e., Dansgaard–Oeschger cycles). Drilling of Lake Petén Itzá will recover the cores needed to test this inference.

The seismic facies and architecture of Sequence B document a different mode of sedimentation than seen in the units above. Sequence B fills topographic depressions in the basement and is less draping than overlying units, indicating the prominent role of lateral transport processes (e.g., turbidites from underflows) that focus sediment into deeper parts of the basin. Sediments at the base of this unit directly overlie basement and reflect the time of initial basin formation and lake filling.

The bathymetry (i.e., steep northern slope and shelving southern shore) of Petén Itzá's basin reflects asymmetric faulting along its northern and southern shores. In the south, a series of basin-parallel faults with low displacements is observed on the seismic data, whereas in the north, a distinct normal fault occurs that has been identified at the surface (Vinson, 1962). This fault pattern created a half-graben structure, which, along with the limestone bedrock and enhanced water flow paths along the faults, was overprinted by dissolution processes. Both tectonism and karstification led to the highly irregular bedrock morphology that typifies the entire Petén region. Lack of faulting in the lacustrine sediment record implies no major neotectonic activity.

5. Conclusions

Seismic surveys of Lake Petén Itzá, Guatemala, provided bathymetric data and information on type,

thickness and depositional processes of the sediments that fill the basin. Long piston cores sampled the upper sequences and were used to "groundtruth" the seismic stratigraphy.

1. The bathymetric survey revealed a maximum water depth of 160 m, which extends 50 m below sea level. This makes Lake Petén Itzá the deepest lake in lowland Central America. Unlike shallower lakes in the region, it likely held water even during full glacial periods when arid climate persisted.
2. Seismic data show a fault-controlled, highly irregular bedrock morphology that is generally asymmetric, indicating a half-graben structure. The tectono-karstic origin of the lake basin (e.g., polje) is a consequence of faulting, enhanced by dissolution of the limestone bedrock.
3. The sediment package overlying basement is of variable thickness and partially infills bedrock depressions. Several basins contain up to 100 m of sediment. Maximum thickness may exceed this amount in the deepest part of the basin where bedrock could not be imaged with the seismic source. Seismic stratigraphic analysis revealed four major seismic sequences overlying basement that are separated by unconformities. These sequences constitute an important sediment archive for reconstruction of Late Quaternary climate and environmental change in the lowland Neotropics.
4. We recognized a persistent buried paleoshoreline on seismic profiles throughout the basin at ~56 m below present lake level. Piston cores taken along a depth transect recovered Late Glacial paleosols landward, and gypsum deposits basinward of the paleoshoreline. This geomorphologic and sedimentologic evidence demonstrates that lake level at the end of the last glacial period was ~56 m lower, implying that Lake Petén Itzá's volume was reduced by ~87% relative to present. The youngest seismic Sequence T was deposited during the flooding of the basin that began at the Pleistocene/Holocene boundary (~10.2 cal kyr BP), which led to a highstand that continues at present.
5. A conceptual model explains the three upper seismic stratigraphic sequences as being a consequence of lake level fluctuations induced by glacial-to-interglacial climate changes on orbital time scales. During glacial periods of the Late Pleistocene, low lake levels caused erosional unconformities that define seismic sequence boundaries, which are traceable throughout the basin. In contrast, full or intermediate interglacial periods are marked by high lake level and by basinwide lacustrine sedimentation. Future recovery of the complete sediment package will ultimately enable us to date the older sequences and test this conceptual model. These long cores will also yield a continuous Late Quaternary paleoclimate record for the lowland Neotropics.

Acknowledgements

We thank Arturo Godoy and Roan McNab of the Wildlife Conservation Society for facilitating fieldwork. Drs. Margaret and Michael Dix (Universidad del Valle de Guatemala) and their many students (Lucía Corral, Oscar Juarez, Gabriela Ponce, Rodolfo Valdez, Julia Quiñones, Liseth Perez, Laura Rodriguez, and Jacobo Blijdenstein) provided help in the field. We are grateful to the Consejo Nacional de Areas Protegidas (CONAP) for logistical assistance during fieldwork. The Limnological Research Center (LRC) at the University of Minnesota supplied the Kullenberg coring system. We thank Douglas W. Schnurrenberger, Jason H. Curtis, David G. Buck, and Michael F. Rosenmeier for help during coring operations. Thomas P. Guilderson (Lawrence Livermore Laboratory) provided radiocarbon dates. The Swiss Embassy (Guatemala City), Sr. Antonio Ortiz (Flores) and Franz Sperisen (Camino Real Tikal) supported the logistics of the fieldwork. The manuscript profited from constructive reviews of Marc de Batist and from an anonymous reviewer. This work was supported by Swiss National Science Foundation grant 620-066113 and ETH Zürich grant 0-43882-99, as well as US National Science Foundation (NSF) grant ATM-0117148.

References

Adams, K.D., Wesnousky, S.G., 1998. Shoreline processes and the age of the Lake Lahontan highstand in the Jessup Embayment, Nevada. GSA Bulletin 110, 505–524.

Ariztegui, D., Anselmetti, F.S., Seltzer, G., Kelts, K., D'Agostino, K., 2000. Identifying paleoenvironmental change across South and North America using high-resolution seismic stratigraphy in

lakes. In: Markgraf, V. (Ed.), Interhemispheric Climate Linkages: Present and Past Interhemispheric Climate Linkages in the Americas and their Societal Effects. Academic Press, pp. 227–240.

Binford, M.W., Brenner, M., Whitmore, T.J., Higuera-Gundy, A., Deevey Jr., E.S., Leyden, B., 1987. Ecosystems, paleoecology and human disturbance in subtropical and tropical America. Quaternary Science Review 6, 115–128.

Bradbury, J.P., Leyden, B.W., Salgado-Labouriau, M.L., Lewis Jr., W.M., Schubert, C., Binford, M.W., Frey, D.G., Whitehead, D.R., Weibezahn, F.H., 1981. Late Quaternary environmental history of Lake Valencia, Venezuela. Science 214, 1299–1305.

Brenner, M., 1994. Lakes Salpetén and Quexil, Petén, Guatemala, Central America. In: Kelts, K., Gierlowski-Kordesch, E. (Eds.), Global Geological Record of Lake Basins, vol. 1. Cambridge University Press, Cambridge, UK, pp. 377–380.

Brenner, M., Curtis, J.H., Higuera-Gundy, A., Hodell, D.A., Jones, G.A., Binford, M.W., Dorsey, K.T., 1994. Lake Miragoane, Haiti (Caribbean). In: Kelts, K., Gierlowski-Kordesch, E. (Eds.), Global Geological Record of Lake Basins, vol. 1. Cambridge University Press, Cambridge, UK, pp. 403–405.

Brenner, M., Rosenmeier, M.F., Hodell, D.A., Curtis, J.H., 2002. Paleolimnology of the Maya lowlands: long-term perspectives on interactions among climate, environment, and humans. Ancient Mesoamerica 13, 141–157.

Covich, A.P., 1976. Recent changes in molluscan diversity of a large tropical lake (Lago de Petén, Guatemala). Limnology and Oceanography 21, 51–59.

Curtis, J.H., Hodell, D.A., 1993. An isotopic and trace element study of ostracods from Lake Miragoane, Haiti. A 10.5 kyr record of paleosalinity and paleotemperature changes in the Caribbean. In: Swart, P.K., Lohmann, K.C., McKenzie, J., Savin, S. (Eds.), Climate Change in Continental Isotopic Records, Geophysical Monograph, vol. 78. American Geophysical Union, Washington D.C., pp. 135–152.

Curtis, J.H., Brenner, M., Hodell, D.A., Balser, R.A., Islebe, G.A., Hoogheimstra, H., 1998. A multi-proxy study of Holocene environmental change in the Maya Lowlands of Petén, Guatemala. Journal of Paleolimnology 19, 139–159.

Curtis, J.H., Brenner, M., Hodell, D.A., 1999. Climate change in Lake Valencia Basin, Venezuela, ~12600 yr BP to present. The Holocene 9, 609–619.

De Batist, M., Van Rensbergen, P., Back, S., Klerkx, J., 1996. Structural framework, sequence stratigraphy and lake level variations in the Livingstone Basin (northern Lake Malawi): first results of a high-resolution reflection seismic study. In: Johnson, T., Odada, E. (Eds.), The Limnology, Climatology and Paleoclimatology of the East African Lakes. Gordon and Breach Pub. Inc., Newark, pp. 509–521.

Deevey Jr., E.S., Rice, D.S., Rice, P.M., Vaughan, H.H., Brenner, M., Flannery, M.S., 1979. Mayan urbanism: impact on a tropical karst environment. Science. New Series 206/4416, 298–306.

Deevey, E.S., Brenner, M., Flannery, M.S., Yezdani, G.H., 1980. Lakes Yaxha and Sacnab, Petén Guatemala: limnology and hydrology. Archiv für Hydrobiologie 57, 419–460.

Deevey, E.S., Brenner, M., Binford, M.W., 1983. Paleolimnology of the Petén Lake District, Guatemala: III. Late Pleistocene and Gamblian environments of the Maya area. Hydrobiologia 103, 211–216.

Fedotov, A., Kazansky, A.Y., Tomurhuu, D., Matasova, G., Ziborova, G., Zhelenznyakova, T., Voroboyova, S., Phedorin, M., Goldberg, E., Oyunchimeg, T., Narantsetseg, T., Vologina, E., Yuldashev, A., Kalugin, I., Tomurtogoo, O., Grachev, M., 2004. A 1-Myr record of paleoclimates from Lake Khubsugul, Mongolia. EOS 85/40, 387–390.

Gilli, A., Anselmetti, F.S., Ariztegui, D., Bradbury, J.P., Kelts, K., Markgraf, V., McKenzie, J.A., 2001. Tracking abrupt climate change in the southern hemisphere: a seismic stratigraphic study of Lago Cardiel, Argentina (49°S). Terra Nova 13 (6), 443–448.

Gilli, A., Anselmetti, F.S., Ariztegui, D., Beres, M., McKenzie, J.A., Markgraf, V., 2005. Seismic stratigraphy, buried beach ridges and contourite drifts: the Late Quaternary history of the closed Lago Cardiel basin, Argentina (49°S). Sedimentology 52, 1–23.

Hillesheim, M.B., Hodell, D.A., Leyden, B.W., Brenner, M., Curtis, J.H., Anselmetti, F.S., Ariztegui, D., Buck, D.G., Guilderson, T.P., Rosenmeier, M.F., Schnurrenberger, D.W., 2005. Climate change in lowland Central America during the late deglacial and early Holocene. Journal of Quaternary Science 20, 363–376.

Hodell, D.A., Curtis, J.H., Jones, G.A., Higuera-Gundy, A., Brenner, M., Binford, M.W., Dorsey, K.T., 1991. Reconstruction of Caribbean climate change over the past 10,500 years. Nature 352, 790–793.

Ibbeken, H., Warnke, D.A., 2000. The Hanaupah-Fan shoreline deposit at Tule Spring, a gravelly shoreline deposit of Pleistocene Lake Manly, Death Valley, California, USA. Journal of Paleolimnology 23, 439–447.

Komatsu, G., Brantingham, P.J., Olsen, J.W., Baker, V.R., 2001. Paleoshoreline geomorphology of Boon Tsagan Nuur, Tsagaan Nuur and orog Nuur, the Valley of Lakes, Mongolia. Geomorphology 39, 83–98.

Lemmin, U., 1998. Courantologie lémanique. Archives des Sciences et Compte Rendu des séances de la Société de Physique et d'Histoire Naturelle de Genève 51, 103–120.

Leyden, B.W., Brenner, M., Hodell, D.A., Curtis, J.H., 1993. Late Pleistocene climate in the central American lowlands. In: Swart, P.K., Lohmann, K.C., McKenzie, J., Savin, S. (Eds.), Climate Change in Continental Isotopic Records, Geophysical Monograph, vol. 78. American Geophysical Union, Washington D.C., pp. 165–178.

Leyden, B.W., Brenner, M., Hodell, D.A., Curtis, J.H., 1994. Orbital and internal forcing of climate on the Yucatan Peninsula for the past ca. 36 ka. Palaeogeography, Palaeoclimatology, Palaeoecology 109, 193–210.

Piovano, E., Ariztegui, D., Damatto Moreira, S., 2002. Recent environmental changes in Laguna Mar Chiquita (central Argentina): a sedimentary model for a highly variable saline lake. Sedimentology 49, 1371–1384.

Rosenmeier, M.F., Hodell, D.A., Brenner, M., Curtis, J.H., 2002. A 4000-year lacustrine record of environmental change in the southern Maya Lowlands, Petén, Guatemala. Quaternary Research 57, 183–190.

Sack, D., 2001. Shoreline and basin configuration techniques in paleolimnology. In: Last, W.M., Smol, J.P. (Eds.), Tracking

Environmental Change Using Lake Sediments, Volume 1, Basin Analysis, Coring and Chronological Techniques. Kluwer Academic Publishers, Dordrecht, The Netherlands, pp. 49–71.

Scholz, C.A., 2001. Applications of seismic sequence stratigraphy in lacustrine basins. In: Last, W.M., Smol, J.P. (Eds.), Tracking Environmental Change Using Lake Sediments, Volume 1, Basin Analysis, Coring and Chronological Techniques. Kluwer Academic Publishers, Dordrecht, The Netherlands, pp. 7–22.

Scholz, C.A., Rosendahl, B.R., 1988. Low lake stands in lakes Malawi and Tanganyika, East Africa, delineated with multifold seismic data. Science 240, 1645–1648.

Seltzer, G.O., Baker, P., Cross, S., Dunbar, R., Fritz, S., 1998. High-resolution seismic profiles from Lake Titicaca, Peru–Bolivia: evidence for Holocene aridity in the tropical Andes. Geology 26, 167–170.

Stuiver, M., Reimer, P.J., 1993. Extended C data base and revised Calib 3.0 C age calibration program. Radiocarbon 35, 35–65.

Stuiver, M., Reimer, P.J., Bard, E., Beck, J.W., Burr, G.S., Hughen, K.A., Kromer, B., McCormac, G., van der Plicht, J., Spurk, M., 1998. INTCAL98 radiocarbon age calibration, 24,000–0 cal BP. Radiocarbon 40, 1041–1083.

Thompson, T.A., 1992. Beach-ridge development and lake level variation in southern Lake Michigan. Sedimentary Geology 80, 305–318.

Vail, P.R., Mitchum, R.M., Thompson III, S., 1977. Cycles of relative changes of sea level. In: Payton, C.E. (Ed.), Seismic Stratigraphy—Applications to Hydrocarbon Exploration, Memoir, vol. 26. American Association of Petroleum Geologists, pp. 83–97.

Vinson, G.L., 1962. Upper cretaceous and tertiary stratigraphy of Guatemala. Bulletin of the American Association of Petroleum Geologists 46, 425–456.

Wattrus, N.J., Rausch, D.E., 2001. A preliminary survey of relict shoreface-attached sand ridges in western Lake Superior. Marine Geology 179, 163–177.